

Immune Correlates of Protection From West Nile Virus Neuroinvasion and Disease

Jessica B. Graham,¹ Jessica L. Swarts,¹ Sunil Thomas,² Kathleen M. Voss,² Aimee Sekine,² Richard Green,² Renee C. Ireton,² Michael Gale,² and Jennifer M. Lund^{1,3}

¹Vaccine and Infectious Disease Division, Fred Hutchinson Cancer Research Center, and ²Center for Innate Immunity and Immune Disease, Department of Immunology, School of Medicine, and ³Department of Global Health, School of Medicine and School of Public Health, University of Washington, Seattle, Washington

Background. A challenge to the design of improved therapeutic agents and prevention strategies for neuroinvasive infection and associated disease is the lack of known natural immune correlates of protection. A relevant model to study such correlates is offered by the Collaborative Cross (CC), a panel of recombinant inbred mouse strains that exhibit a range of disease manifestations upon infection.

Methods. We performed an extensive screen of CC-F1 lines infected with West Nile virus (WNV), including comprehensive immunophenotyping, to identify groups of lines that exhibited viral neuroinvasion or neuroinvasion with disease and lines that remained free of WNV neuroinvasion and disease.

Results. Our data reveal that protection from neuroinvasion and disease is multifactorial and that several immune outcomes can contribute. Immune correlates identified include decreased suppressive activity of regulatory T cells at steady state, which correlates with peripheral restriction of the virus. Further, a rapid contraction of WNV-specific CD8⁺ T cells in the brain correlated with protection from disease.

Conclusions. These immune correlates of protection illustrate additional networks and pathways of the WNV immune response that cannot be observed in the C57BL/6 mouse model. Additionally, correlates of protection exhibited before infection, at baseline, provide insight into phenotypic differences in the human population that may predict clinical outcomes upon infection.

Keywords. Collaborative Cross; immune correlates; neuroinvasion; West Nile virus disease; West Nile virus.

Neuroinvasive infections, including those due to viruses such as West Nile virus (WNV), Zika virus, herpes simplex virus, varicella zoster virus, and human immunodeficiency virus, are a source of a significant portion of the worldwide disease burden. Despite the severity of this public health challenge, available prevention strategies or therapeutic agents are limited for many of these infections. One barrier to the development of new preventive and therapeutic agents is the lack of identified immune correlates of protection from neuroinvasive infection and disease. With improved knowledge about the types of immune responses that can naturally achieve protection from viral invasion of the nervous system, we can next seek to generate or manipulate these protective immune responses to prevent deleterious clinical outcomes.

WNV is one of several neurotropic flaviviruses and can cause disease ranging from a self-limiting febrile illness to an extreme central nervous system (CNS) disease, including meningitis and encephalitis [1, 2]. It is estimated that approximately 20% of infections result in a limited febrile illness, with 1% resulting in a severe

neuroinvasive disease [3]. Studies in the C57BL/6 mouse model of WNV infection have begun to elucidate the immune correlates of protection from infection and have identified aspects of both the innate and adaptive immune responses that orchestrate protection and control of WNV infection [4]. These include induction of RIG-I-like receptor (RLR) pathways and type I interferon (IFN) [5–8], induction of virus-specific immunoglobulin M [9, 10], and generation of WNV-specific CD8⁺ T cells [11]. However, these immune correlates were all identified using the standard inbred C57BL/6 mouse model, which naturally limits the range of immune responses and disease states induced upon infection, owing to the single genotype of the model. The human population, in contrast, is much more diverse, with complex genetic networks and pathways contributing to the diversity in severity of infections, disease outcomes, and immunophenotypes. Rather than limit our study of immune correlates of protection from WNV to hosts with a single genotype, akin to studying a single human with the expectation that it adequately represents the human population, we turned to the Collaborative Cross (CC) mouse model to address the need for a model of increased genetic diversity while maintaining a reproducible, inbred mouse model.

The CC is a population of recombinant inbred mouse strains with high levels of standing genetic variation. The CC strains are derived from 8 founder mouse strains: 5 classical inbred strains and 3 wild-derived strains [12–15]. We have previously shown that the CC can be used to model diversity in human WNV disease states

Received 25 September 2018; editorial decision 19 October 2018; accepted 24 October 2018; published online October 26, 2018.

Correspondence: J. M. Lund, PhD, Fred Hutchinson Cancer Research Center, 1100 Fairview Ave N, E5-110, Seattle, WA 98109 (jlund@fredhutch.org).

The Journal of Infectious Diseases® 2019;219:1162–71

© The Author(s) 2018. Published by Oxford University Press for the Infectious Diseases Society of America. All rights reserved. For permissions, e-mail: journals.permissions@oup.com. DOI: 10.1093/infdis/jiy623

not captured in the B6 model [16, 17] and additionally demonstrated that the CC better represents the large diversity in T-cell immunophenotypes represented in the human population [18]. Here, we use the CC in combination with a mouse model of WNV infection to identify novel innate and adaptive immune correlates of protection from viral neuroinvasion and disease.

METHODS

Mice

CC-RI mice were obtained from the Systems Genetics Core Facility at the University of North Carolina–Chapel Hill (UNC) [19]. F1 hybrid male mice aged 6–8 weeks were transferred from UNC to the University of Washington and housed directly in a biosafety level 2+ laboratory within a specific-pathogen-free barrier facility. Male mice aged 8–10 weeks were used for all experiments, with 3–6 mice per experimental group. Additional details are described in the Supplementary Methods.

Virus and Infection

WNV TX-2002-HC (WN-TX) was propagated as previously described [20]. Mice were subcutaneously inoculated in the rear footpad with 100 plaque-forming units of WN-TX. Mice were monitored daily for morbidity (calculated as the percentage of weight lost from baseline) and clinical disease scores [21].

RNA Extraction and Analysis

Spleen and brain were removed from mice after perfusion, RNA was extracted, and complementary DNA was synthesized as previously described [22]. WNV, *Ifit1*, *Il12b*, *Ifitm1*, and *Ifnb1* expression was detected by SYBR Green real-time quantitative polymerase chain reaction analysis based on the 2- $\Delta\Delta$ CT method and normalized for the individual GAPDH values in each sample. The values represent fold increases in expression as compared to expression in mock-infected mice. For WNV, the values represent the fold increase in signal over an arbitrarily low value in mock-infected mice that represents a virus-null sample.

Flow Cytometry

Following euthanasia, mice underwent perfusion with 10 mL of phosphate-buffered saline to remove any residual intravascular leukocytes, and spleens and brains were prepared for flow cytometry staining as previously described [16–18, 21].

Statistical Analysis

When comparing groups, 2-tailed unpaired Student *t* tests were conducted, with *P* values of <.05 considered significant. Error bars denote standard deviations.

RESULTS

Oas1b Plays a Dominant but Not Exclusive Role in Restricting WNV Neuroinvasion and Disease

A key host genetic factor responsible for resistance to WNV disease is *Oas1b*, with polymorphisms in this gene driving

resistance to flaviviral infections in mice [23, 24]. Within the CC, there are differences in *Oas1b*; while the 5 classic inbred founder strains have identical truncated, “null” (N) sequences (termed “N alleles”) at *Oas1b* due to a premature stop codon, the 3 wild-derived strains all share the functional (F), full-length coding sequence (termed “F alleles”) and thus a larger *Oas1b* linked with resistance to WNV infection [17, 22]. Thus, because of genotypic differences in *Oas1b* within the CC founders, the CC has been used to further examine the effects of *Oas1b* genotype on WNV disease [17, 22]. As part of a large screen of CC-F1 lines to identify novel genes regulating immunity to WNV infection, we infected 110 CC-F1 lines (12 mice/line) with WNV and subsequently assessed weight loss, death, clinical scores, and viral loads of infected mice and uninfected mice (3–6 mice/line). Previously, using data from this screen, we showed that the *Oas1b* genotype plays a role in WNV susceptibility and disease; notably, all mice with an *Oas1b* N/N genotype had symptomatic disease, although the presence of an F allele in heterozygous offspring did not absolutely predict protection against disease [22]. Thus, for our analysis of immune correlates of protection from viral neuroinvasion and disease, we focused on lines with an *Oas1b* heterozygous genotype, to search for immune correlates of protection beyond *Oas1b*.

Thus, we examined data from all 110 lines that were screened with WNV infection and had an *Oas1b* heterozygous genotype (F/N or N/F) that (1) could restrict WNV to the periphery and showed no signs of disease (termed “peripheral restriction” [PR] and defined as brain PCR values \leq 2-fold greater than those for mock-infected mice on days 7 and 12, weight loss of <5% from baseline, survival, and a clinical score of 0), (2) had WNV present in the brain but no disease (termed “neuroinvasion, no disease” [NND] and defined as brain PCR values \geq 10-fold greater than those for mock-infected mice on days 7 and/or 12, weight loss of <5% from baseline, survival, and a clinical score of 0), or (3) had WNV present in the brain and signs of disease (termed “neuroinvasion with disease” [ND] and defined as brain PCR values \geq 10-fold greater than those for mock-infected mice on days 7 and/or 12, weight loss of >5% from baseline, and/or death, and/or a clinical score of >0; Table 1). By grouping *Oas1b* heterozygous CC-F1 lines in this manner, we can thus use immunophenotypic data from our screen to identify immune correlates of viral peripheral restriction by comparing the PR and NND groups, as well as to identify immune correlates of protection from viral disease by comparing the NND and ND groups.

Distinct Steady-State T-Cell Phenotypes Correlate With Peripheral WNV Restriction

Using data from CC-F1 lines in the PR and NND categories, we examined various T-cell phenotypes before WNV infection to determine if baseline immunophenotypes can predict protection from WNV neuroinvasion (Figure 1). Notably, reduced

Table 1. Characteristics of *Oas1b* Heterozygous Collaborative Cross (CC) F1 Mouse Lines in Disease Categories

Disease Category, CC F1 Line	<i>Oas1b</i> Genotype	Maximum Percentage Weight Loss	Maximum Clinical Score	Mouse Deaths, No.	Brain WNV Load ^a		Neurological Disease Notes
					Day 7	Day 12	
WNV peripheral restriction, no disease ^b							
CC011 × CC042	N/F	0–5	0	0	0.82	0.93	NA
CC013 × CC041	N/F	0–5	0	0	1.45	1.02	NA
CC061 × CC039	N/F	0–5	0	0	1.06	0.88	NA
CC008 × CC010	F/N	0–5	0	0	0.79	1.03	NA
CC046 × CC068	F/N	0–5	0	0	1.82	1.37	NA
CC033 × CC046	N/F	0–5	0	0	0.90	1.18	NA
CC029 × CC027	F/N	0	0	0	0.62	0.93	NA
CC058 × CC022	N/F	0–5	0	0	1.45	0.85	NA
CC006 × CC039	N/F	0–5	0	0	0.53	0.93	NA
CC008 × CC009	F/N	0	0	0	0.62	0.59	NA
WNV neuroinvasion, no disease ^c							
CC004 × CC011	F/N	0–5	0	0	1.54	93.67	NA
CC019 × CC002	F/N	0–5	0	0	1.23	50.08	NA
CC032 × CC017	N/F	0–5	0	0	48.68	10.87	NA
CC012 × CC032	F/N	0–5	0	0	10.82	9.71	NA
CC040 × CC003	N/F	0	0	0	1.89	14.12	NA
CC030 × CC061	F/N	0–5	0	0	34.80	4.55	NA
CC023 × CC025	N/F	0–5	0	0	87.77	23.68	NA
CC038 × CC013	F/N	0–5	0	0	8.78	122.00	NA
CC039 × CC020	F/N	0–5	0	0	1.08	29.06	NA
CC020 × CC008	N/F	0	0	0	2.83	13.55	NA
CC003 × CC062	F/N	0	0	0	0.99	16.76	NA
CC061 × CC025	N/F	0	0	0	10.71	2.41	NA
WNV neuroinvasion with disease ^d							
CC061 × CC026	N/F	≥20	2	4	0.70	8609.88	Paralysis/hind limb weakness
CC016 × CC038	N/F	≥20	1	3	143.89	243.28	NA
CC052 × CC014	N/F	NA	1	4	34.87	138.77	NA
CC055 × CC028	N/F	≥20	1	1	7.99	317.59	NA
CC028 × CC024	F/N	10–20	1	0	8.91	2717.54	NA
CC007 × CC070	N/F	5–10	0	0	3.67	45.39	NA
CC005 × CC038	N/F	NA	4	1	1583.73	12.84	Shaking

Abbreviations: F, functional *Oas1b* coding sequence; N, null *Oas1b* coding sequence; NA, not applicable; PCR, polymerase chain reaction.

^aData are fold increases in signal over an arbitrarily low value in mock-infected mice that represents a virus-null sample.

^bDefined as brain PCR values ≤2-fold greater than those for mock-infected mice on days 7 and 12, weight loss of <5% from baseline, survival, and a clinical score of 0.

^cDefined as brain PCR values ≥10-fold greater than those for mock-infected mice on days 7 and/or 12, weight loss of <5% from baseline, survival, and a clinical score of 0.

^dDefined as brain PCR values ≥10-fold greater than those for mock-infected mice on days 7 and/or 12, weight loss of >5% from baseline, and/or death, and/or a clinical score of >0.

regulatory T-cell (Treg; CD4⁺Foxp3⁺) activation at steady state, in terms of both CTLA-4 and CD44 expression, was associated with peripheral restriction of virus (Figure 1A). Humans infected with WNV have a lower frequency of circulating Tregs when they have symptomatic as compared to asymptomatic disease [25], but samples were not collected prospectively in past studies and so preinfection Treg status in humans has not been assessed.

We next examined baseline T-cell phenotypes in CC-F1 mice with PR or NND after WNV infection. An increased frequency of CD8⁺ T cells and a reduced frequency of CD4⁺ T cells was associated with peripheral restriction of WNV (Figure 1B). Last, a decreased frequency of CD44⁺CD8⁺ or CD44⁺CD4⁺ T cells

was associated with viral peripheral restriction (Figure 1C), perhaps indicating that an increased proportion of naive CD8⁺ and CD4⁺ T cells before infection is advantageous for host WNV peripheral restriction upon challenge.

Innate Immunity and WNV Peripheral Restriction

Previously, we evaluated transcriptional signatures of a subset of *Oas1b* N/F or F/N CC lines and found that particular innate immune signatures can influence biological pathways for WNV control, both in *Oas1b*-dependent and -independent processes [22]. Here, using data from PR and NND CC-F1 lines, we examined a subset of innate immune genes at days 4, 7, and 12 after WNV infection. In the brain, while no virus was detected

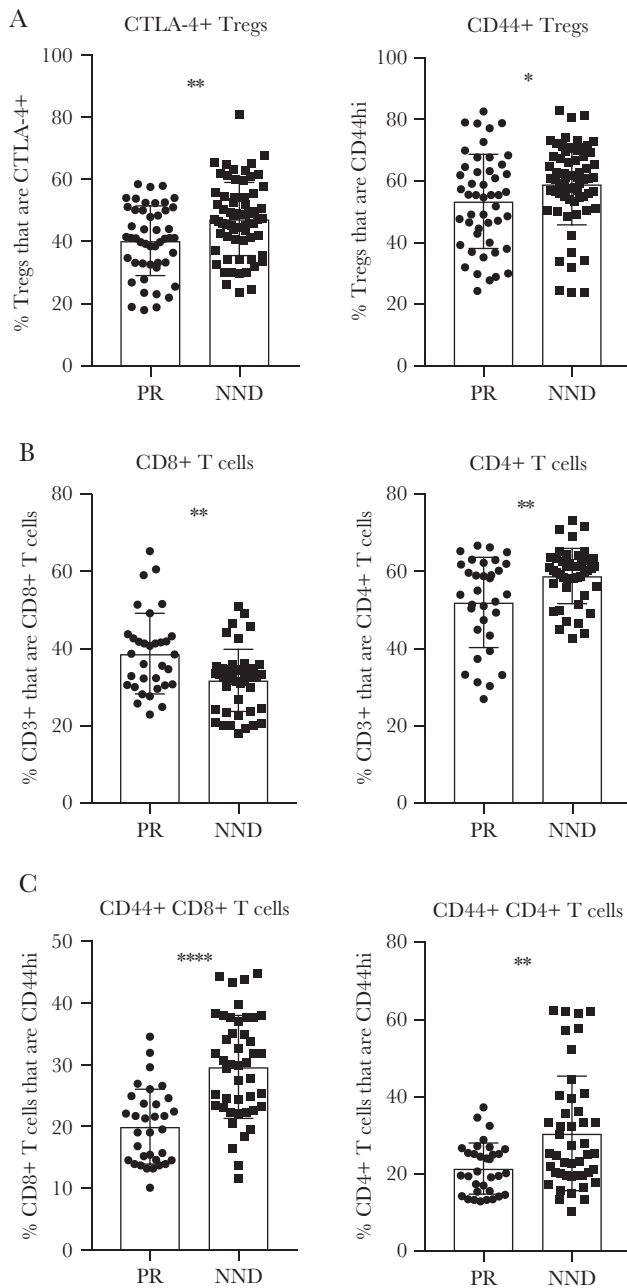


Figure 1. Baseline immune parameters associated with West Nile virus (WNV) peripheral restriction. F1 crosses of Collaborative Cross strains were grouped into peripheral restriction (PR) and neuroinvasion, no disease (NND) categories as defined in “Results” and Table 1. Age-matched male mice were euthanized, and spleens were harvested and prepared for flow cytometry staining to determine the frequency of regulatory T cells (Tregs) expressing CTLA-4 or CD44 (A), the frequency of CD3⁺ T cells that are CD8⁺ T cells or CD4⁺ T cells (B), and the frequency of CD8⁺ and CD4⁺ T cells that express CD44 (C). Statistical significance was determined by the unpaired *t* test. **P* ≤ .05, ***P* ≤ .01, ****P* ≤ .001, and *****P* ≤ .0001.

on day 4 in NND mice, the WNV load increased on day 7 and day 12 after infection, while WNV remained undetectable in PR lines (Figure 2A). In the spleen on day 4 after infection, PR lines had significantly reduced viral titers as compared to NND lines, while both groups achieved viral clearance in the periphery by

day 7 after infection. Perhaps in response to viral invasion to the brain in NND lines (Figure 2A), levels of the innate immune markers IFIT1, IFTM1, IFN- β , and interleukin 12 (IL-12) were significantly increased in the brain in NND lines as compared to PR lines on day 12 (Figure 2B–E). In the spleen, levels of IFITM1 were significantly lower in NND lines as compared to PR lines at the earliest time point measured, day 2 after infection (Figure 2C). This suggests that this decrease in antiviral activity may contribute to a higher viral load in the spleen that can escape the periphery when not controlled early.

Splenic Correlates of WNV Peripheral Restriction

Next, we examined the types of T-cell responses correlated with WNV peripheral restriction by comparing T-cell phenotypes in the PR and NND groups upon WNV infection. On day 7 after infection, a reduced frequency of total and activated CD4⁺ T cells in the spleen correlated with WNV peripheral restriction (Figure 3A). Additionally, a decreased frequency of CXCR3⁺ Tregs in the spleen on day 7 after infection associated with protection from WNV neuroinvasion (Figure 2B). CXCR3 has been shown to mediate T-cell trafficking to the brain during WNV infection [26], and, thus, Tregs may be migrating to the CNS in NND mice to restrict immunopathology due to viral neuroinvasion and the associated T-cell inflammatory response in this tissue upon viral neuroinvasion. Last, we found that an increased frequency of CD73⁺ Tregs in the spleen on day 7 after infection is associated with peripheral restriction (Figure 3C). CD73 produced by Tregs has been shown to downregulate nuclear factor κ B activation in effector T cells, reducing the release of proinflammatory cytokines [27], which could here serve to limit the antiviral response and associated immunopathology in these lines that achieve peripheral restriction of the virus.

Baseline Immune Parameters Correlated With WNV-Induced Disease Upon Infection

Many CC-F1 lines experience viral neuroinvasion upon WNV infection but do not exhibit clinical signs of disease. We next wanted to examine what differentiates these NND lines from ND lines, where there is virus in the brain on day 7 or day 12, as well as clinical disease symptoms (Table 1). Starting with baseline immune parameters, we compared NND and ND CC-F1 lines and found that having an increased frequency of activated, CD44⁺ or β 1-integrin-expressing Tregs in the spleen before infection correlated with protection from disease (Figure 4A and 4B). β 1-integrin, a component of VLA-4, has been reported to be necessary for T-cell recruitment across the blood brain barrier [28]. Notably, β 1 integrin has been shown to be important for T-cell entry into the CNS, and so we predict that β 1 integrin-expressing Tregs are able to migrate to the CNS to play an immunosuppressive role.

Next, we assessed conventional T-cell phenotypes within the spleen at baseline to determine if there are predictive signatures

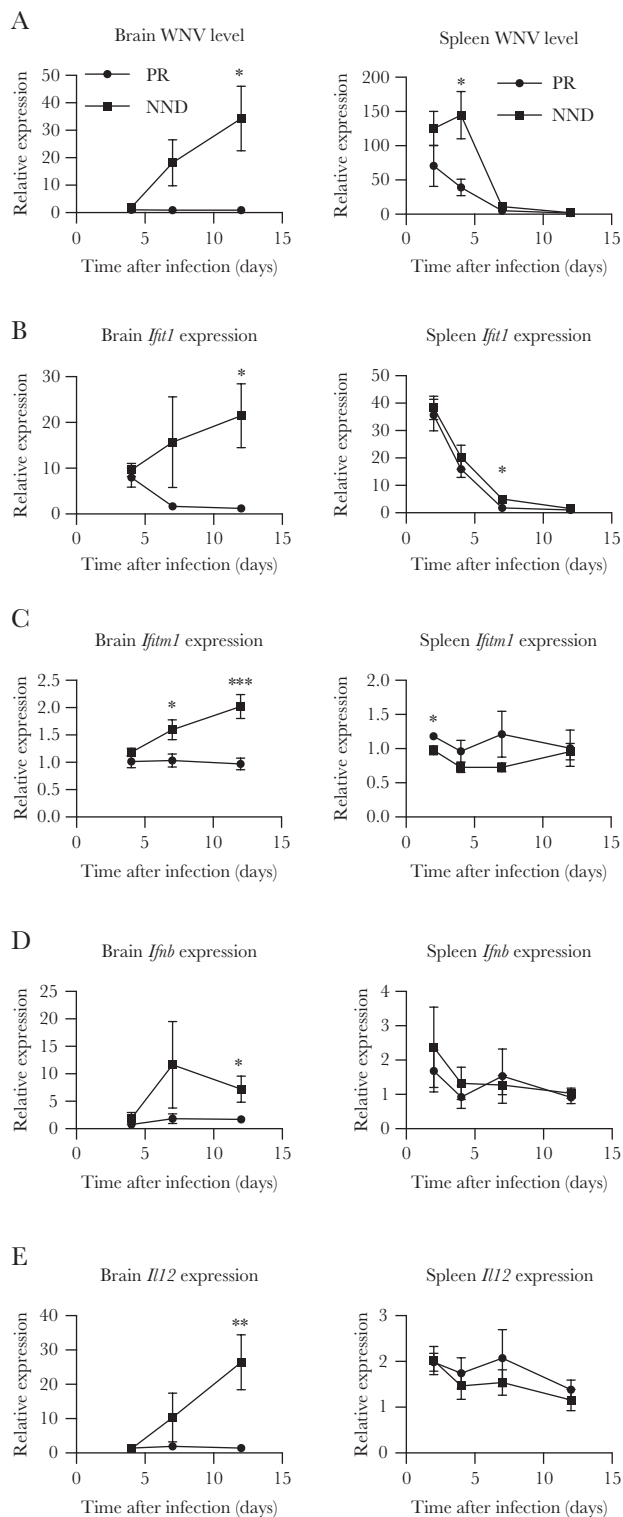


Figure 2. Innate immune response correlates of virus restriction to the periphery. F1 crosses of Collaborative Cross strains were grouped into peripheral restriction (PR) and neuroinvasion, no disease (NND) categories as defined in “Results” and Table 1. Cohorts of mice were infected with 100 plaque-forming units of West Nile virus (WNV) by subcutaneous injection in the rear footpad. At the indicated times after infection, age-matched male mice were euthanized, and spleens and brains were harvested and prepared for quantitative real-time polymerase chain reaction analysis to quantify the WNV load (A) and *Ifit1* (B), *Ifitm1* (C), *Ifnb* (D), and *Il12* (E) expression. Statistical significance at each time point was determined by the unpaired *t* test. * $P \leq .05$, ** $P \leq .01$, *** $P \leq .001$, and **** $P \leq .0001$.

of disease upon infection. An increased frequency of activated, CD44⁺CD4⁺ T cells in the spleen at baseline correlated with protection from disease upon WNV infection (Figure 4C). Additionally, a reduced baseline frequency of CD3⁺ T cells within the spleen correlated with protection from neuroinvasive disease symptoms (Figure 4D). As a frequency of total cells, a decreased fraction of the compartment being comprised of CD3⁺ T cells may result in an increase in the frequency of myeloid cells, which are necessary for early viral control [29, 30].

Innate Immunity and Protection From WNV-Induced Disease

To next identify innate immune correlates of protection from WNV-induced disease, we compared innate immune response parameters in NND and ND lines. There was no significant difference in the quantity of WNV within the brain and spleen of NND and ND groups (Figure 5A), despite the difference in disease (Table 1). Thus, the viral burden was unlikely the sole driver of disease. Overall, we found greater activation of the innate immune response in the spleen and brain in ND lines (Figure 5B–E). Notably, there was a dramatic and significant increase in IFIT1, IFITM1, and IFN- β levels in the brain on day 12 after infection of ND lines as compared to NND lines, suggesting that decreased innate immune activation in the brain at this later time point may be an immune correlate of protection from WNV-induced disease.

Splenic and Brain T-Cell Responses and Protection From Disease

Finally, we compared WNV-induced adaptive immune responses in NND and ND lines to identify T-cell correlates of protection from WNV-induced disease. In the spleen on day 7 after infection, we observed that an increased frequency of Tregs expressing activation and migration markers CD44, ICOS, and CXCR3 was associated with protection from disease (Figure 6A). In contrast, a reduced frequency of CD73⁺ Tregs in the spleen on day 7 after infection correlated with protection from WNV-induced disease (Figure 6B). When we examined splenic CD8⁺ and CD4⁺ T-cell phenotypes in NND and ND lines, we found that an increased frequency of WNV-specific CD8⁺ T cells (Figure 6C) and an increased frequency of CXCR3⁺CD4⁺ T cells (Figure 6D) in the spleen on day 7 after infection correlated with protection from disease.

Last, we compared T-cell responses in the brain in NND and ND lines to identify immune correlates of protection from disease present within the nervous system. On day 7 after infection, there is a reduced frequency of $\beta 1$ -integrin-expressing migratory Tregs in NND lines as compared to ND lines (Figure 6E). Further, we observed an increased frequency of WNV-specific CD8⁺ T cells within the brain of NND lines as compared to ND lines on day 7 after infection (Figure 6F), although by day 12 after infection, there was an increased frequency of WNV-specific CD8⁺ T cells in ND lines as compared to NND lines (Figure 6G). Thus, it appears that delayed trafficking or accumulation of WNV-specific CD8⁺ T cells within the brain is correlated with WNV-induced disease.

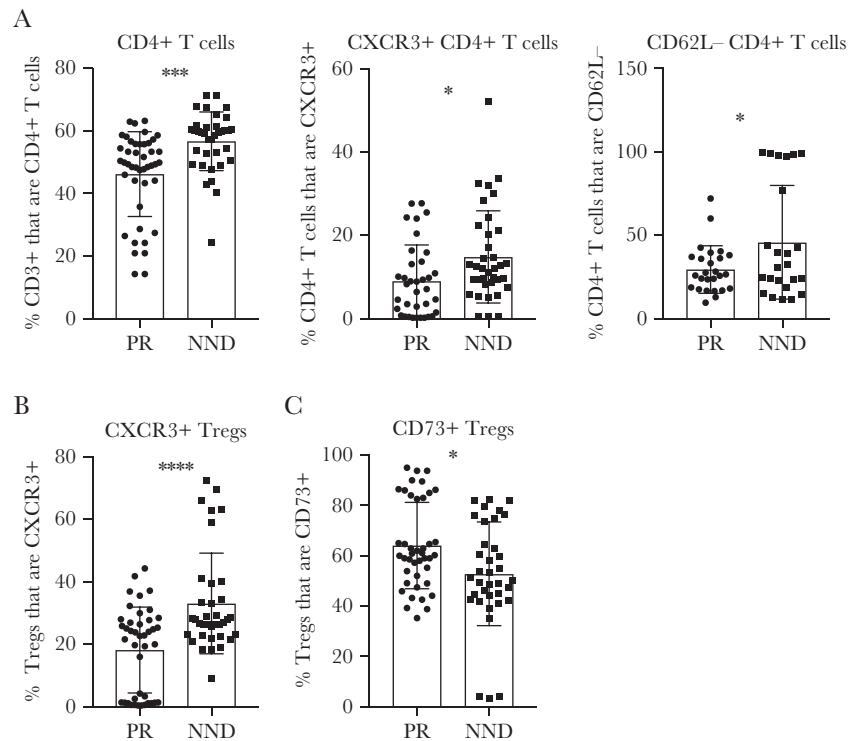


Figure 3. Peripheral T-cell responses linked to West Nile virus (WNV) restriction from the central nervous system. F1 crosses of Collaborative Cross strains were grouped into peripheral restriction (PR) and neuroinvasion, no disease (NND) categories as defined in “Results” and Table 1. Cohorts of mice were infected with 100 plaque-forming units of WNV by subcutaneous injection in the rear footpad. On day 7 after infection, age-matched male mice were euthanized, and spleens were harvested and prepared for flow cytometry staining to determine the frequency of CD3+ cells that are CD4+ T cells, the frequency of CD4+ T cells expressing CXCR3 or not expressing CD62L (A), the frequency of regulatory T cells (Tregs) not expressing CXCR3 (B), or the frequency of Tregs expressing CD73 (C). Statistical significance was determined by the unpaired *t* test. **P* ≤ .05, ***P* ≤ .01, ****P* ≤ .001, and *****P* ≤ .0001.

DISCUSSION

We used the CC in combination with a mouse model of WNV infection to identify novel innate and adaptive immune correlates of protection from both infection of the CNS, as well as from WNV-induced disease (Supplementary Table 1). At steady state, a reduced frequency of CTLA-4-expressing Tregs was associated with peripheral restriction of virus (Figure 1A). This suggests that reduced Treg-mediated suppression may assist in prevention of WNV neuroinvasion, perhaps by allowing an unleashed and immediate robust immune response upon infection that can then control virus within the periphery. In line with this hypothesis, early innate immune activity in the spleen, in the form of a slight but significant increase in the IFITM1 level on day 2 after infection, was correlated with protection from viral neuroinvasion (Figure 2C). On day 7 after infection, we found that reduced splenic CD4+ T-cell frequency and activation was associated with protection from neuroinvasion (Figure 3A), although this may be an indicator of reduced viral loads in the spleen (Figure 2A) that thereby does not necessitate such a robust T-cell response, rather than an indication that CD4+ T-cell activity promotes neuroinvasion. Of note, an increased frequency of CD73+ Tregs in the spleen on day 7 after WNV infection correlated with peripheral restriction of virus,

suggesting that the CD73-mediated mode of Treg suppression may play an important role in preventing spread of WNV into the nervous system. As it has previously been shown that Treg activity is required during viral infections to allow for appropriate generation and migration of immune effector cells to the site of infection [31–33], it is possible that this augmented Treg expression of CD73 plays a role in coordinating effective anti-WNV immunity. It is also possible that Tregs help to curtail the immune response to WNV via a CD73-dependent mechanism upon viral clearance in the spleen (Figure 2A). In the latter case, this Treg function is indicative of a role in restraining an antipathogen immune response that has effectively performed its function, rather than a role in protecting from neuroinvasion.

When viral neuroinvasion does occur, a distinct set of immune parameters correlate with protection from disease upon WNV infection. While reduced Treg activity at baseline appears beneficial in terms of preventing WNV neuroinvasion, maintenance of Tregs in a state of reduced activation is not advantageous in all clinical settings. Indeed, an increased frequency of activated splenic Tregs correlated with protection from disease in mice with neuroinvasive infection (Figure 4A and 4B). Similarly, 7 days after infection, an increased frequency of activated Tregs correlated with protection from disease

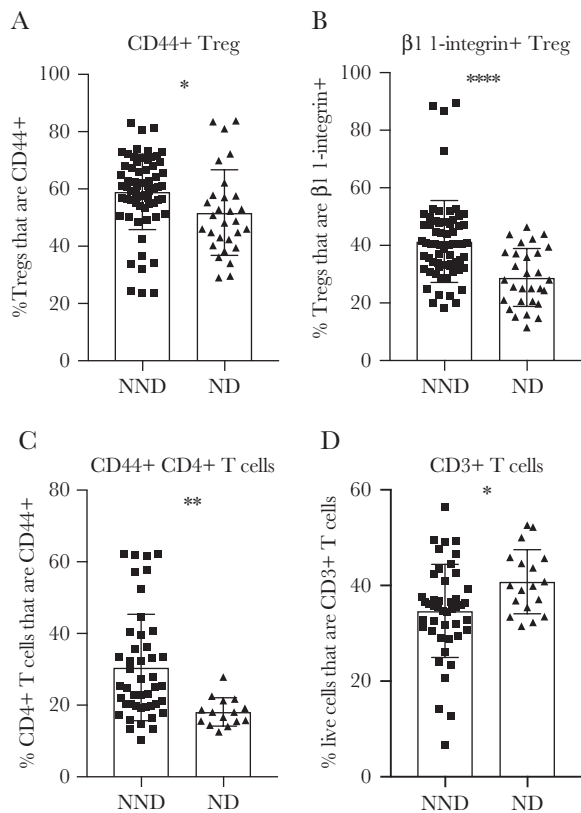


Figure 4. Baseline immune parameters can predict West Nile virus–induced disease upon infection. F1 crosses of Collaborative Cross strains were grouped into neuroinvasion, no disease (NND) and neuroinvasion with disease (ND) categories as defined in “Results” and Table 1. Age-matched male mice were euthanized, and spleens were harvested and prepared for flow cytometry staining to determine the frequency of regulatory T cells (Tregs) expressing CD44 (A), the frequency of Tregs expressing $\beta 1$ -integrin (B), the frequency of CD4⁺ T cells expressing CD44 (C), and the frequency of live splenocytes expressing CD3 (D). Statistical significance was determined by the unpaired *t* test. **P* ≤ .05, ***P* ≤ .01, ****P* ≤ .001, and *****P* ≤ .0001.

(Figure 6A). We hypothesize that this increased Treg activity assists in preventing tissue damage due to infection-induced immunity. Indeed, Tregs have been shown to limit proinflammatory cytokine production to preserve nonrenewing cell types in nonlymphoid tissues [34]. Additionally, tissue-resident Tregs have been shown to rapidly respond to inflammation and tissue damage to repair and restore function [35]. Interestingly, however, reduced frequencies of CD73⁺ Tregs correlated with protection from disease, again pointing out that CD73 may represent a unique mechanism of Treg-mediated activity upon WNV infection.

In addition to differences in baseline Treg phenotypes, we also observed altered preinfection conventional T-cell phenotypes that correlated with eventual protection from disease upon WNV infection. Notably, a reduced frequency of CD3⁺ T cells within the spleen or, conversely, an increased frequency

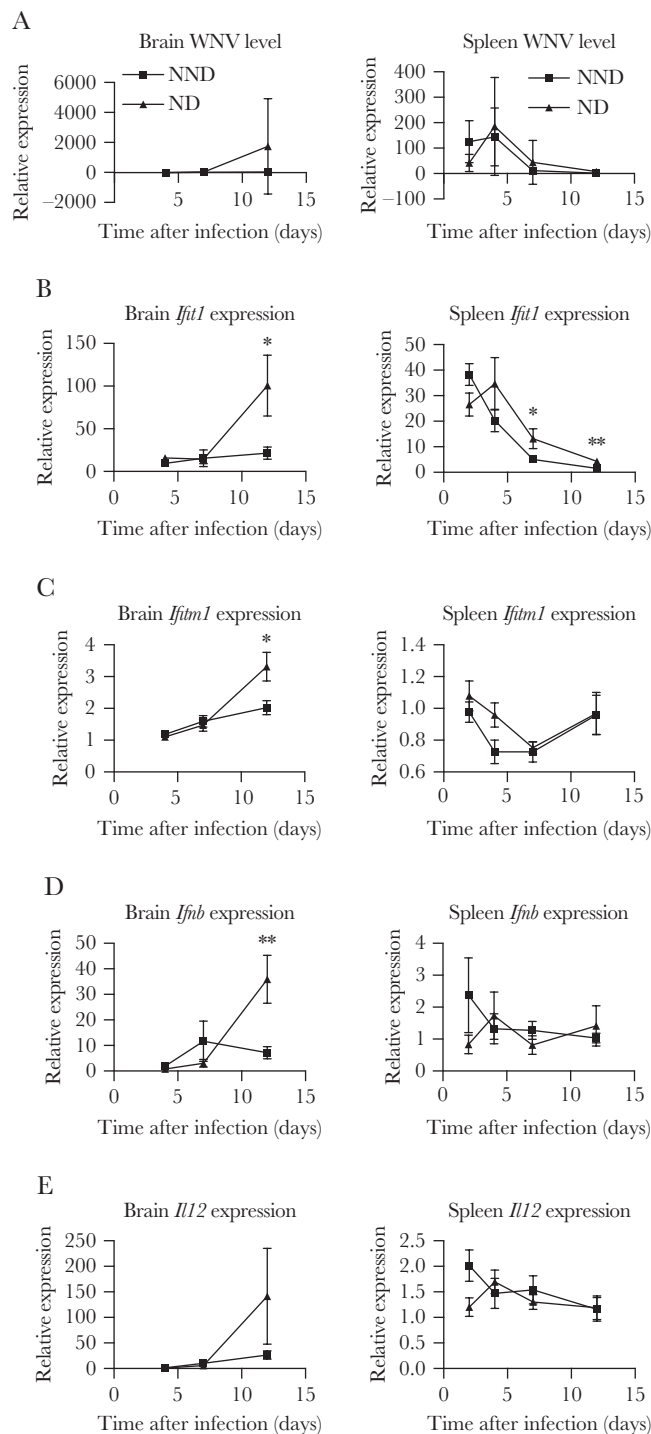


Figure 5. Innate immune correlates of protection from West Nile virus (WNV) disease. F1 crosses of Collaborative Cross strains were grouped into neuroinvasion, no disease (NND) and neuroinvasion with disease (ND) categories as defined in “Results” and Table 1. Cohorts of mice were infected with 100 plaque-forming units of WNV by subcutaneous injection in the rear footpad. At the indicated times after infection, age-matched male mice were euthanized, and spleens and brains were harvested and prepared for quantitative real-time polymerase chain reaction analysis to quantify the WNV load (A) and *Ifit1* (B), *Ifim1* (C), *Ifnb* (D), and *Il12* (E) expression. Statistical significance at each time point was determined by the unpaired *t* test. **P* ≤ .05, ***P* ≤ .01, ****P* ≤ .001, and *****P* ≤ .0001.

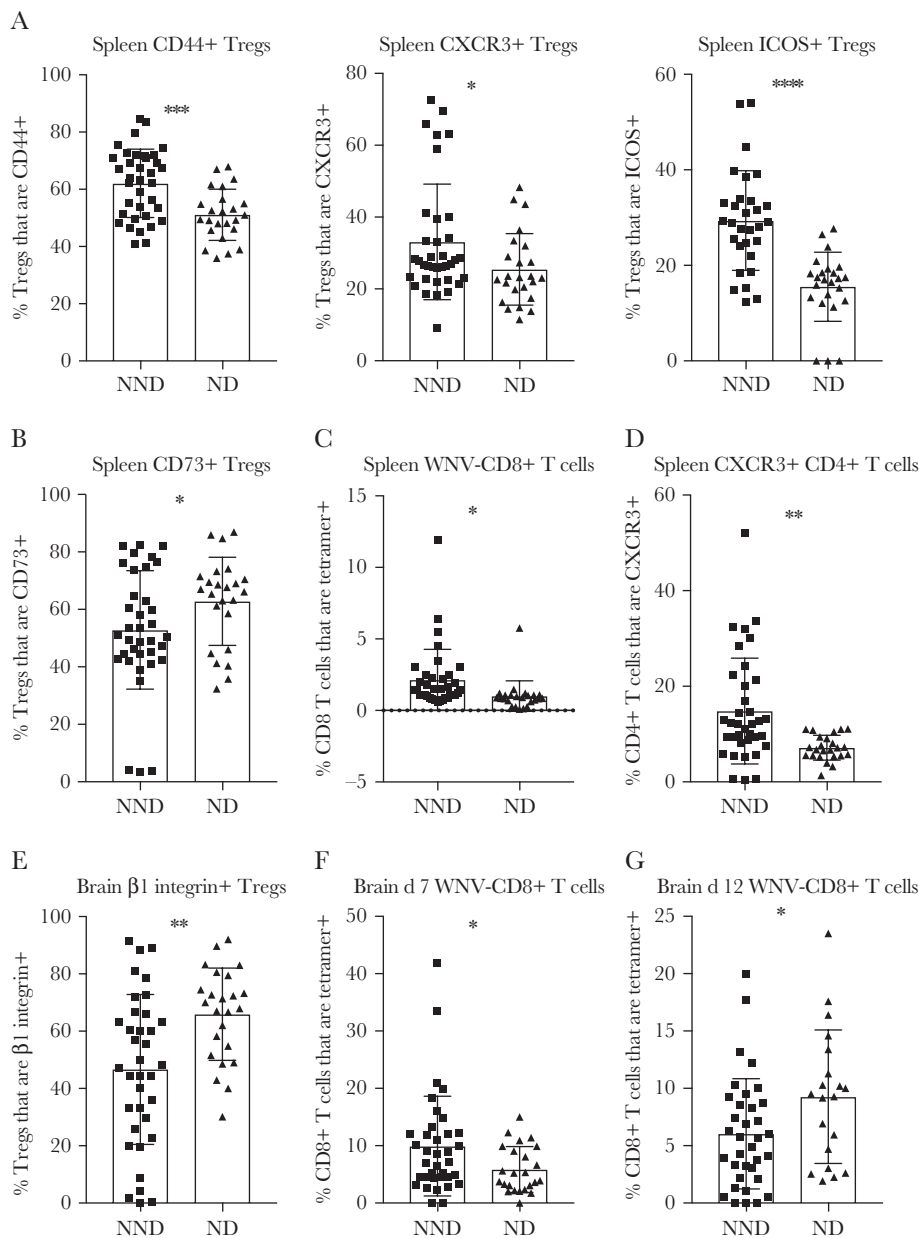


Figure 6. Splenic and central nervous system T-cell responses correlate with increased disease outcomes after West Nile virus (WNV) infection. F1 crosses of Collaborative Cross strains were grouped into neuroinvasion, no disease (NND) and neuroinvasion with disease (ND) categories as defined in “Results” and Table 1. Cohorts of mice were infected with 100 plaque-forming units of WNV by subcutaneous injection in the rear footpad. At day 7 or 12 after infection, age-matched male mice were euthanized, and spleens and brains were harvested and prepared for flow cytometry staining to determine the frequency of splenic regulatory T cells (Tregs) expressing CD44, CXCR3, or ICOS on day 7 after infection (A), the frequency of splenic Tregs expressing CD73 on day 7 after infection (B), the frequency of splenic CD8⁺ T cells expressing tetramer on day 7 after infection (C), the frequency of splenic CD4⁺ T cells expressing CXCR3 on day 7 after infection (D), the frequency of brain Tregs expressing β1-integrin on day 7 after infection (E), and the frequency of brain CD8⁺ T cells expressing tetramer on day 7 (F) and day 12 after infection (G). Statistical significance was determined by the unpaired *t* test. **P* ≤ .05, ***P* ≤ .01, ****P* ≤ .001, and *****P* ≤ .0001.

of CD3⁻ cells, was associated with protection from disease (Figure 4D). Because CD3⁻ cells include innate immune cells such as antigen-presenting cells and natural killer cells, as well as B cells, it is possible that tipping the balance in favor of one or more of these cell types gives an advantage to mice upon infection with WNV, although additional screening of CC mice is required to profile immune cell types not analyzed in

the present study. In addition to the CD3⁺ T-cell phenotype, we found that an increased frequency of CD44⁺CD4⁺ T cells in the spleen at baseline correlated with protection from disease upon WNV infection (Figure 4C). Antigen-experienced memory CD44⁺CD4⁺ T cells could perhaps participate in the anti-WNV immune response, even in the absence of cognate antigen, in a bystander-mediated fashion and, thus, assist in early pathogen

control and thereby curtail onset of disease. An examination of the potential role for bystander-mediated T-cell activity in preventing viral neuroinvasion and disease is needed to determine if such cells can play an active role during WNV infection.

From our analysis of immunophenotypes after infection in mice with neuroinvasion without (NND lines) or with (ND lines) disease, we also determined that late and robust innate immune activity within the brain correlates with disease (Figure 5). Again, however, it is possible that this immune activity may be either a driver of disease or an indicator of continued viral replication with the nervous system (Figure 5A); further study is required to establish cause and effect. In terms of adaptive immunity, we identified that an increased frequency of WNV-specific CD8⁺ T cells in the spleen and brain on day 7 after infection correlated with protection from disease (Figure 6C and 6F). This is consistent with the notion that a robust and early WNV-specific CD8⁺ T-cell response can effectively control virus replication without excessive immune-mediated pathology that could result in disease. Further, a reduced and perhaps contracted frequency of WNV-specific CD8⁺ T cells in the brain on day 12 after infection correlated with protection from disease (Figure 6G). We hypothesize that the prolonged CD8⁺ T-cell response in the brain is at least partially responsible for disease, likely through immunopathology. Indeed, it is possible that the increased Treg activity observed in the spleen at day 7 after infection in mice without disease (Figure 6A) assisted in this timely control of the WNV-specific CD8⁺ T-cell response.

A clear advantage of this study is that use of CC mice, rather than examination of retrospectively collected human specimens, allowed us to consistently examine immunity, viral pathogenesis, and clinical disease following primary infection with WNV at specific time points after infection. Although studies in female mice and in humans are required to confirm these correlates of protection from WNV infection and disease, use of this large screen of CC mice has allowed for identification of novel immune correlates not previously identified using C57BL/6 mice or human samples that were not prospectively collected at preinfection time points. In the continued design of improved therapeutic agents for and strategies to prevent neuroinvasive infection and disease, consideration of these natural immune correlates of protection from neuroinvasion and disease that we have identified may assist in selection of new drug targets. Additionally, this knowledge improves our understanding of how effective immunity to WNV must be optimally coordinated to both clear the infection and minimize immunopathology and disease.

Supplementary Data

Supplementary materials are available at *The Journal of Infectious Diseases* online. Consisting of data provided by the authors to benefit the reader, the posted materials are not copyedited and are the sole responsibility of the authors, so questions or comments should be addressed to the corresponding author.

Notes

Acknowledgments. We thank our collaborators in the Systems Immunogenetics Group for helpful discussions and generation of mice, particularly Ginger Shaw, for generating the RIX mice used in this study.

J. B. G., M. G., and J. M. L. designed the research studies; J. B. G., J. L. S., S. T., K. M. V., and A. S. conducted experiments and acquired data; J. B. G., J. L. S., S. T., K. M. V., A. S., R. G., and R. I. analyzed data; and J. B. G. and J. M. L. wrote the first draft of the manuscript; and all authors read the manuscript and contributed editorial suggestions.

Financial support. This work was supported by the National Institutes of Health (grant U19AI100625 [project 3] to M. G. and J. M. L.).

Potential conflicts of interest. All authors: No reported conflicts of interest. All authors have submitted the ICMJE Form for Disclosure of Potential Conflicts of Interest. Conflicts that the editors consider relevant to the content of the manuscript have been disclosed.

References

1. Colpitts TM, Conway MJ, Montgomery RR, Fikrig E. West Nile virus: biology, transmission, and human infection. *Clin Microbiol Rev* **2012**; 25:635–48.
2. Samuel MA, Diamond MS. Pathogenesis of West Nile virus infection: a balance between virulence, innate and adaptive immunity, and viral evasion. *J Virol* **2006**; 80:9349–60.
3. Diamond MS, Mehlhop E, Oliphant T, Samuel MA. The host immunologic response to West Nile encephalitis virus. *Front Biosci (Landmark Ed)* **2009**; 14:3024–34.
4. Suthar MS, Diamond MS, Gale M Jr. West Nile virus infection and immunity. *Nat Rev Microbiol* **2013**; 11:115–28.
5. Daffis S, Samuel MA, Keller BC, Gale M Jr, Diamond MS. Cell-specific IRF-3 responses protect against West Nile virus infection by interferon-dependent and -independent mechanisms. *PLoS Pathog* **2007**; 3:e106.
6. Daffis S, Samuel MA, Suthar MS, Keller BC, Gale M Jr, Diamond MS. Interferon regulatory factor IRF-7 induces the antiviral alpha interferon response and protects against lethal West Nile virus infection. *J Virol* **2008**; 82:8465–75.
7. Errett JS, Suthar MS, McMillan A, Diamond MS, Gale M Jr. The essential, nonredundant roles of RIG-I and MDA5 in detecting and controlling West Nile virus infection. *J Virol* **2013**; 87:11416–25.
8. Samuel MA, Whitby K, Keller BC, et al. PKR and RNase L contribute to protection against lethal West Nile virus infection by controlling early viral spread in the periphery and replication in neurons. *J Virol* **2006**; 80:7009–19.
9. Diamond MS, Shrestha B, Marri A, Mahan D, Engle M. B cells and antibody play critical roles in the immediate defense of disseminated infection by West Nile encephalitis virus. *J Virol* **2003**; 77:2578–86.

10. Diamond MS, Sitati EM, Friend LD, Higgs S, Shrestha B, Engle M. A critical role for induced IgM in the protection against West Nile virus infection. *J Exp Med* **2003**; 198:1853–62.
11. Wang Y, Lobigs M, Lee E, Koskinen A, Müllbacher A. CD8(+) T cell-mediated immune responses in West Nile virus (Sarafend strain) encephalitis are independent of gamma interferon. *J Gen Virol* **2006**; 87:3599–609.
12. Churchill GA, Airey DC, Allayee H, et al.; Complex Trait Consortium. The Collaborative Cross, a community resource for the genetic analysis of complex traits. *Nat Genet* **2004**; 36:1133–7.
13. Collaborative Cross C. The genome architecture of the Collaborative Cross mouse genetic reference population. *Genetics* **2012**; 190:389–401.
14. Keane TM, Goodstadt L, Danecek P, et al. Mouse genomic variation and its effect on phenotypes and gene regulation. *Nature* **2011**; 477:289–94.
15. Roberts A, Pardo-Manuel de Villena F, Wang W, McMillan L, Threadgill DW. The polymorphism architecture of mouse genetic resources elucidated using genome-wide resequencing data: implications for QTL discovery and systems genetics. *Mamm Genome* **2007**; 18:473–81.
16. Graham JB, Swarts JL, Wilkins C, et al. A mouse model of chronic West Nile virus disease. *PLoS Pathog* **2016**; 12:e1005996.
17. Graham JB, Thomas S, Swarts J, et al. Genetic diversity in the collaborative cross model recapitulates human West Nile virus disease outcomes. *MBio* **2015**; 6:e00493–15.
18. Graham JB, Swarts JL, Mooney M, et al. Extensive homeostatic T cell phenotypic variation within the Collaborative Cross. *Cell Rep* **2017**; 21:2313–25.
19. Welsh CE, Miller DR, Manly KF, et al. Status and access to the Collaborative Cross population. *Mamm Genome* **2012**; 23:706–12.
20. Suthar MS, Ma DY, Thomas S, et al. IPS-1 is essential for the control of West Nile virus infection and immunity. *PLoS Pathog* **2010**; 6:e1000757.
21. Graham JB, Swarts JL, Lund JM. A mouse model of West Nile virus infection. *Curr Protoc Mouse Biol* **2017**; 7:221–35.
22. Green R, Wilkins C, Thomas S, et al. Oas1b-dependent immune transcriptional profiles of West Nile virus infection in the Collaborative Cross. *G3 (Bethesda)* **2017**; 7:1665–82.
23. Bigam AW, Buckingham KJ, Husain S, et al. Host genetic risk factors for West Nile virus infection and disease progression. *PLoS One* **2011**; 6:e24745.
24. Courtney SC, Di H, Stockman BM, Liu H, Scherbik SV, Brinton MA. Identification of novel host cell binding partners of Oas1b, the protein conferring resistance to flavivirus-induced disease in mice. *J Virol* **2012**; 86:7953–63.
25. Lanteri MC, O'Brien KM, Purtha WE, et al. Tregs control the development of symptomatic West Nile virus infection in humans and mice. *J Clin Invest* **2009**; 119:3266–77.
26. Zhang B, Chan YK, Lu B, Diamond MS, Klein RS. CXCR3 mediates region-specific antiviral T cell trafficking within the central nervous system during West Nile virus encephalitis. *J Immunol* **2008**; 180:2641–9.
27. Romio M, Reinbeck B, Bongardt S, Hüls S, Burghoff S, Schrader J. Extracellular purine metabolism and signaling of CD73-derived adenosine in murine Treg and Teff cells. *Am J Physiol Cell Physiol* **2011**; 301:C530–9.
28. Man S, Ubogu EE, Ransohoff RM. Inflammatory cell migration into the central nervous system: a few new twists on an old tale. *Brain Pathol* **2007**; 17:243–50.
29. Steinbrink K, Mahnke K, Grabbe S, Enk AH, Jonuleit H. Myeloid dendritic cell: from sentinel of immunity to key player of peripheral tolerance? *Hum Immunol* **2009**; 70:289–93.
30. Swiecki M, Gilfillan S, Vermi W, Wang Y, Colonna M. Plasmacytoid dendritic cell ablation impacts early interferon responses and antiviral NK and CD8(+) T cell accrual. *Immunity* **2010**; 33:955–66.
31. Lund JM, Hsing L, Pham TT, Rudensky AY. Coordination of early protective immunity to viral infection by regulatory T cells. *Science* **2008**; 320:1220–4.
32. Ruckwardt TJ, Bonaparte KL, Nason MC, Graham BS. Regulatory T cells promote early influx of CD8+ T cells in the lungs of respiratory syncytial virus-infected mice and diminish immunodominance disparities. *J Virol* **2009**; 83:3019–28.
33. Soerens AG, Da Costa A, Lund JM. Regulatory T cells are essential to promote proper CD4 T-cell priming upon mucosal infection. *Mucosal Immunol* **2016**; 9:1395–406.
34. Burzyn D, Benoist C, Mathis D. Regulatory T cells in non-lymphoid tissues. *Nat Immunol* **2013**; 14:1007–13.
35. Arpaia N, Green JA, Moltedo B, et al. A distinct function of regulatory T cells in tissue protection. *Cell* **2015**; 162:1078–89.